ELSEVIER

Journal of Fluids and Structures 19 (2004) 159–170

JOURNAL OF FLUIDS AND STRUCTURES

www.elsevier.nl/locate/jnlabr/yjfls

Phase-averaged characteristics of flow around a circular cylinder under acoustic excitation control

N. Fujisawa*, G. Takeda, N. Ike

Department of Mechanical and Production Engineering, Niigata University, 8050 Ikarashi 2, Niigata 950-2181, Japan

Received 15 April 2003; accepted 6 October 2003

Abstract

The influence of internal acoustic excitation on the aerodynamic performance of a circular cylinder in a uniform flow is studied by the phase-averaged measurements of fluid forces and flow fields around the cylinder. The experimental results indicate that the mean drag as well as the fluctuating lift are reduced by the acoustic excitation control from a slit on a circular cylinder. The phase-averaged PIV measurements at the vortex shedding frequency show that the periodic and fluctuating velocities are suppressed in the wake of the controlled cylinder, which indicates the influence of acoustic excitation on the vortex shedding and the corresponding reduction in the fluid forces on the circular cylinder. On the other hand, the phase-averaged flow field at the excitation frequency of unstable shear layer, which is four times larger than the vortex shedding frequency, indicates the formation of discrete vortices along the shear layer of the cylinder wake. The interaction of these vortices with the cylinder wake causes the reduction in the cross-correlations of velocity fluctuations in the flow field, which results in the attenuation of the vortex shedding phenomenon in the cylinder wake.

Keywords: Flow-induced vibration; Flow measurement; Flow control; PIV; Vortex shedding; Acoustic excitation

1. Introduction

The flow control around a bluff body structure in a stream has been a topic of interest in recent years in relation to the engineering problems of flow-induced vibration and noise. Therefore, the flow field around and the wake behind the bluff body structure have been studied in a literature both for its fundamental interest and for industrial application. The outcomes of such studies are summarized in some review papers by Bearman (1984), Naudascher (1987), Griffin and Hall (1991) and others. It is well known that the flow control techniques of a bluff body structure can be categorized into passive and active control techniques. The passive technique uses the vortex suppression devices such as the axial slats, the splitter plate and so on (Blevins, 1990). On the other hand, the active technique can be applied to the bluff body structure without the modification of geometrical configuration. The active control of vortex shedding is carried out by using the external forces, which are often produced by the acoustic excitation (Blevins, 1985; Ffowcs Williams and Zhao, 1989; Hsiao and Shyu, 1991; Amitay et al., 1997; Fujisawa and Takeda, 2003), the oscillatory motion of the cylinder (Tokumaru and Dimotakis, 1991; Filler et al., 1991; Warui and Fujisawa, 1996; He et al., 2000; Fujisawa et al., 2001; Shiels and Leonard, 2001; Srinivas and Fujisawa, 2003), the blowing and suction (Park et al., 1994; Gunzburger and Lee, 1996) and others. These approaches are becoming more attractive with the advance of computer technology in combination with the digital signal processing technique and the intelligent sensing and

*Corresponding author. Tel./fax: +81-25-262-6726.
E-mail address: fujisawa@eng.niigata-u.ac.jp (N. Fujisawa).

0889-9746/$ - see front matter
doi:10.1016/j.jfluidstructs.2003.10.004

actuator techniques. Among these active controls, the internal acoustic technique will provide a basis of an intelligent control methodology of a bluff body wake for the industrial applications.

The active control of vortex shedding using the internal acoustic excitation was first introduced by Hsiao and Shyu (1991). They investigated the influence of acoustic excitation on the aerodynamic performance of a cylinder, where the acoustic excitation was introduced internally to the flow over a circular cylinder through a slit with a loud speaker. Later, Amitay et al. (1997) studied the surface pressure distributions around a circular cylinder under internal excitation by using fluidic actuators and found a drag reduction of 25% at higher Reynolds number, Re = 75500. Recently, Fujisawa and Takeda (2003) investigated the mean fluid forces on a circular cylinder under acoustic excitation control by measuring the time-averaged pressure distributions over the cylinder. The result indicates that the mean drag is reduced up to 30% at Reynolds number 9000. They also measured the distributions of mean and periodic velocities around the cylinder using a standard PIV system and showed that the near-wake velocity profile was considerably modified by the acoustic excitation control.

The purpose of the present experiment is to study the influence of acoustic excitation control on the fluctuating fluid forces of a circular cylinder and to explore the mechanism of the flow control under the acoustic excitation by using phase-averaged PIV measurements. The PIV measurements are carried out at the vortex shedding frequency and at the acoustic excitation frequency to study the periodic variations in the cylinder wake.

2. Experimental apparatus and procedures

2.1. Experimental set-up

A schematic illustration of the flow control by acoustic excitation is shown in Fig. 1. A circular cylinder of diameter d ($=50$ mm) is placed in a uniform flow of velocity U_0 ($=2.6$ m/s). Therefore, the Reynolds number is Re ($=U_0 d/\nu$) $=9000$, where ν is the kinematic viscosity of the fluid. The acoustic excitation is provided from the inside of the cylinder to the flow over the cylinder through a slit. The flow field under the acoustic excitation can be described by non-dimensional parameters, such as the forcing Strouhal number $S_f (= fd/U_0)$, the velocity amplitude $V_r (= v/U_0)$, and the Reynolds number Re, where f is a frequency of the excitation, v is a amplitude of excitation velocity through the slit. According to the previous experiments by Fujisawa and Takeda (2003), the drag force acting on the cylinder is reduced by up to 30%, when the nondimensional parameters are set to $S_f = 4S_{f0}$ and $V_r = 1.5$ at Re = 9000, where S_{f0} ($= f_0 d/U_0$) $= 0.21$ is a natural Strouhal number of vortex shedding. It is noted that the slit is located at $\beta = 90^\circ$ to meet with the condition of maximum drag reduction. Therefore, the present experiment is carried out under the optimum combinations of control parameters for drag reduction ($S_f = 4S_{f0}$, $V_r = 1.5$, $\beta = 90^\circ$), the results of which are compared with the uncontrolled case.

The present experiments were carried out in an open-jet type wind tunnel, which has a cross-sectional area of 500×500 mm. The nonuniformity of the free-stream velocity was 1% and the streamwise turbulence intensity was 0.8% of the free-stream velocity. The test cylinder was supported by two vertical side-walls of the test-section, which are made of transparent materials for visualization purposes. Two end-plates are attached on both ends of the cylinder to maintain the two-dimensionality of the flow field, whereas the top and bottom boundary of the test-section are made free. The acoustic excitations are provided by two loud-speakers (300 W), which are attached on both sides of the cylinder. The width of the slit over the cylinder is 0.4 mm and has a spanwise length of 400 mm. The loud-speaker was driven by a sinusoidal wave-generator in combination with the power amplifier. Details of the experimental test section

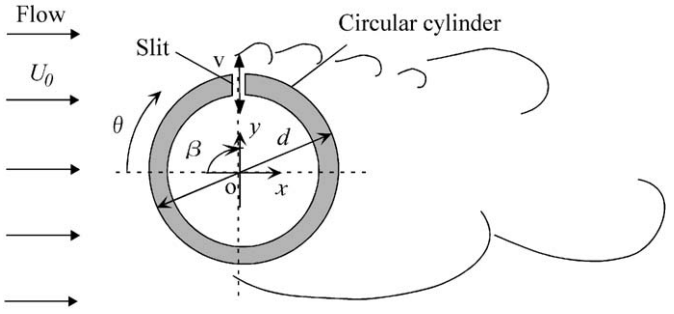

Fig. 1. Illustration of circular cylinder under acoustic excitation control.

are the same as Fujisawa and Takeda (2003) except for the structure of the test cylinder, which is modified to detect the pressure fluctuation over the cylinder surface.

2.2. Measurement of phase-averaged fluid forces

The fluctuating fluid forces on a circular cylinder are evaluated from the measurement of phase-averaged pressure distribution over the cylinder surface. The pressure distribution at a certain phase of vortex shedding is measured by detecting two pressure signals over the cylinder surface simultaneously: the first at the measurement point and the other is at the reference point at angle $\theta = 270^\circ$. It is noted that the pressure signal is taken from pressure holes of 0.8 mm in diameter distributed over the cylinder circumference around the mid-plane, connected by a stainless-steel tube of 2.4 mm in diameter to a pressure transducer of strain-gauge type fixed outside the cylinder; 31 pressure holes are distributed over the cylinder surface at every 11.25° except for the slit location.

The frequency response of the measuring system including the tubing is found to be flat up to 200 Hz, which is high enough for the present measurement of phase-averaged pressure distributions (Fujisawa et al., 1998). The output signals from the pressure transducers are analyzed in the computer to obtain the phase-averaged pressure distribution over the cylinder surface. The phase-averaged fluid forces are evaluated by integrating the pressure distribution over the cylinder surface. The uncertainty in the measurement of fluid forces is estimated to be 5% at 95% coverage.

2.3. Phase-averaged PIV measurement

The phase-averaged flow field around a circular cylinder under the acoustic excitation was measured by particle image velocimetry (PIV). The tracer particles of smoke were supplied from the smoke generator through the inlet of the blower of the wind tunnel, to visualize the flow around the circular cylinder. Illumination was provided by a light sheet (2 mm in thickness) from the double pulsed Nd:YAG laser, which emits 532 nm wavelength light at a pulse width 5 ns with a pulse rate 15 Hz for each laser. The laser was operated at the pulse energy of 50 mJ. The flow observation is made by a monochrome digital CCD camera, which has a spatial resolution of 1008×1018 pixels with 8 bits in gray level. The camera is operated in a double exposure mode, so that two sequential images are captured in a short time interval.

The phase-averaged PIV measurements of the flow field were carried out with reference to the vortex shedding signal and the acoustic excitation signal, respectively. The block diagram of the measurement is shown in Fig. 2. The reference signal of vortex shedding is taken from the pressure signal on the lower side of the cylinder surface ($\theta = 270^\circ$). The signal is detected by a pressure transducer of strain-gauge type and is band-pass-filtered at the vortex shedding frequency ($f = 12$ Hz). The filtered signal is processed in a digital signal processor to generate a pulse signal for conditional sampling at a certain phase of vortex shedding. The phase $\varphi = 0^\circ$ of the vortex shedding is evaluated in reference to the filtered pressure signal, when the sign of the signal changes from the negative to the positive. A certain phase φ is counted in a computer by using a timer function, where the period of vortex shedding is estimated from previous cycles of the pressure signal. The same technique was used for the conditional sampling at the frequency of acoustic excitation. However, the signal for acoustic excitation was directly supplied to the digital signal processor in this case, because the acoustic excitation signal was generated in a computer as a sinusoidal wave. The conditional sampling signal triggers the pulse controller for the operation of the CCD camera and the laser illumination. Therefore,

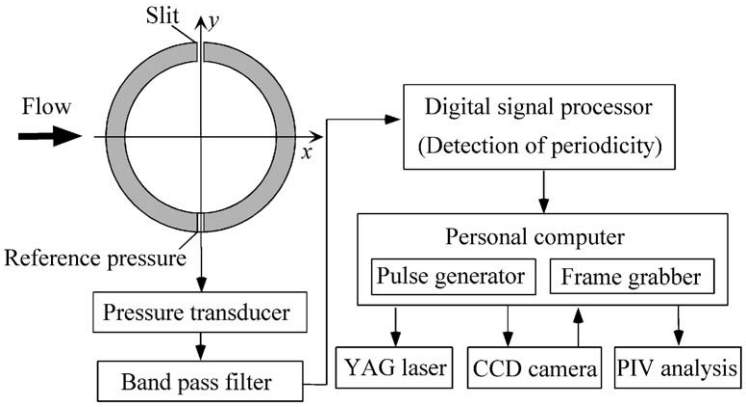

Fig. 2. Block diagram of phase-averaged PIV measurement.

two sequential images are captured in the frame grabber, when the conditional sampling signal is supplied to the CCD camera. The delay time between the two successive laser pulses was set to 80 μs in the present experiment.

The target flow area in the cylinder wake has dimensions of 100 mm × 100 mm, so that the spatial resolution of the captured images is about 0.1 mm/pixel. The flow images are stored on the frame memory of the computer to obtain 300 instantaneous velocity distributions at a fixed phase of vortex shedding, which are used for the evaluation of the phase-averaged flow characteristics around the circular cylinder. The algorithm of velocity measurement is based on the gray-level difference method for the cross-correlation calculation between the two successive images. This algorithm works well with a similar uncertainty level as the direct cross-correlation algorithm, but with less computational time (Kaga et al., 1994). The sizes of the interrogation window and the search window were set to 30 pixel × 30 pixel and 44 pixel × 44 pixel, respectively, which combination was found to minimize the appearance of erroneous vectors, with a reasonable spatial resolution. The sub-pixel interpolation process was incorporated into the analysis to improve the accuracy of the velocity measurement. The uncertainty interval of the velocity measurement was estimated to be 3% at 95% coverage.

3. Results and discussions

3.1. Pressure distribution and fluid forces

Fig. 3 shows the distributions of phase averaged pressure coefficient C_p over a circular cylinder with and without the acoustic excitation control, which are plotted against the angle θ at four typical phase angles of vortex shedding: $\varphi = 0°, 90°, 180°, 270°$. The pressure coefficient C_p is defined by $C_p = 2(p - p_\infty)/\rho U_0^2$, where p is a pressure, p_∞ is the free-stream pressure, and ρ is the density of the fluid. It is noted that the phase angle ϕ is defined as the angle where the periodic pressure changes from the negative to the positive. The pressure distribution over the uncontrolled cylinder in Fig. 3(a) indicates that the pressure coefficient C_p behind the cylinder varies periodically with respect to the phase angle ϕ, which indicates the cyclic formation of vortices in the wake of the cylinder. When the acoustic excitation control is applied to the flow over the cylinder (Fig. 3(b)), the pressure distribution behind the cylinder increases and the periodic variations are almost removed. These results indicate that the mean drag force is reduced and the vortex shedding from a circular cylinder is weakened by the acoustic excitation control. It is noted that the mean pressure distribution around the cylinder obtained from the phase-averaged measurement agrees with the time-averaged measurements by Fujisawa and Takeda (2003).

Fig. 4 shows the drag and lift forces on the circular cylinder with and without acoustic excitation control, which are evaluated from the measurement of phase-averaged pressure distribution at the vortex shedding frequency. The drag and lift coefficients are defined by $C_d(= 2F_x/\rho U_0^2)$ and $C_l(= 2F_y/\rho U_0^2)$, respectively, where F_x and F_y are streamwise and normal fluid forces acting on the cylinder, respectively. For the uncontrolled cylinder, the drag coefficient C_d has two peaks in each cycle of vortex shedding, while the lift coefficient shows one peak. These features agree with the well-known behavior of vortex shedding from a circular cylinder in uniform flow (Drescher, 1956). When the acoustic excitation control is applied to the cylinder, the oscillation amplitudes of the drag and lift coefficients are considerably reduced and the distributions become uniform with respect to the phase variations. However, the periodicity of C_l under control (Strouhal number $St = 0.20$) is very close to that of the uncontrolled case ($St = 0.21$), which indicates that the natural frequency of vortex shedding is not so influenced by the acoustic excitation control. The change in the Strouhal number by rotational oscillation in the present experiment is smaller than that of Hsiao and Shyu (1991), who found the Strouhal number $St = 0.20$ for the controlled case and 0.22 for the uncontrolled case. The present result also indicates that the mean drag, as well as the fluctuating lift, are reduced by the acoustic excitation control. However, a small value of mean lift is observable in the lift distribution due to the asymmetrical slit location for the control. It is noted that the mean fluid forces in the present phase-averaged measurement agree closely with the time-averaged measurements by Fujisawa and Takeda (2003) under the same control parameters.

3.2. Flow around uncontrolled cylinder

The phase-averaged PIV measurements are made in the flow field around the uncontrolled cylinder to understand the variation of the flow field with respect to the phases of vortex shedding. Fig. 5(a)–(d) shows the phase-averaged velocity magnitude $\sqrt{U^2 + V^2}/U_0$ and the velocity vectors around the uncontrolled cylinder at four phase angles of vortex shedding: $\phi = 0°, 90°, 180°, 270°$. Here, U and V are streamwise and normal velocities, respectively, and x and y are respectively the streamwise and normal distances from the center of a circular cylinder. The velocity distribution at phase angle $\phi = 0°$ corresponds to the pressure field, where the pressure behind the cylinder is almost uniform and

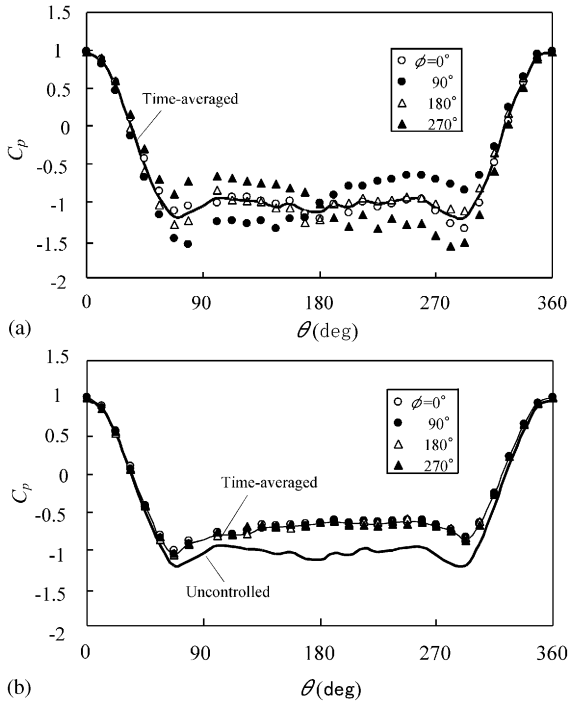

Fig. 3. Phase-averaged pressure distribution over circular cylinder. (a) Uncontrolled case, (b) controlled case.

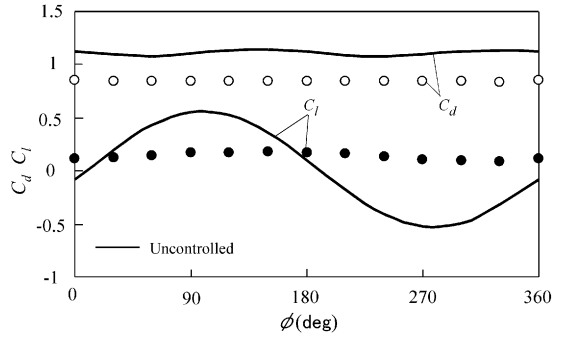

Fig. 4. Variations of drag and lift coefficients with respect to phase angle of vortex shedding.

decreases on the upper side ($\theta = 90°$) and increases on the lower side ($\theta = 270°$) as shown in Fig. 3(a). Therefore, the high velocity region is just starting to form on the upper side of the cylinder and is leaving from the lower side. On the other hand, the wake region downstream of the cylinder ($x/d = 1 - 2$) is deflected to the lower side of the cylinder, which indicates the memory effect of the velocity distribution in a previous time ($\phi = 270°$), where the high velocity region on the upper side of the cylinder dominates over that on the lower side. With an increase in phase angle to $\phi = 90°$, the high velocity region over the lower side of the cylinder moves downstream and that over the upper side grows in size near the cylinder, which indicate the generation of a high pressure region on the lower side and of low pressure region on the upper side of the cylinder. In this case, the wake region ($x/d = 1 - 2$) is deflected to the upper side due to the larger region of high velocity on the lower side and the smaller region on the upper side. These variations of the flow field continue with further increases in the phase angles to $\phi = 180°$ and 270°, which shows the periodic oscillation of the wake velocity profile. It is noted that the variations of the flow field on the uncontrolled cylinder is consistent with those of the pressure distributions on the cylinder surface in Fig. 3(a).

The corresponding phase-averaged velocity fluctuations around the uncontrolled cylinder are given in Fig. 6, where u and v are streamwise and normal velocity fluctuations, respectively. The distributions of velocity fluctuations vary with

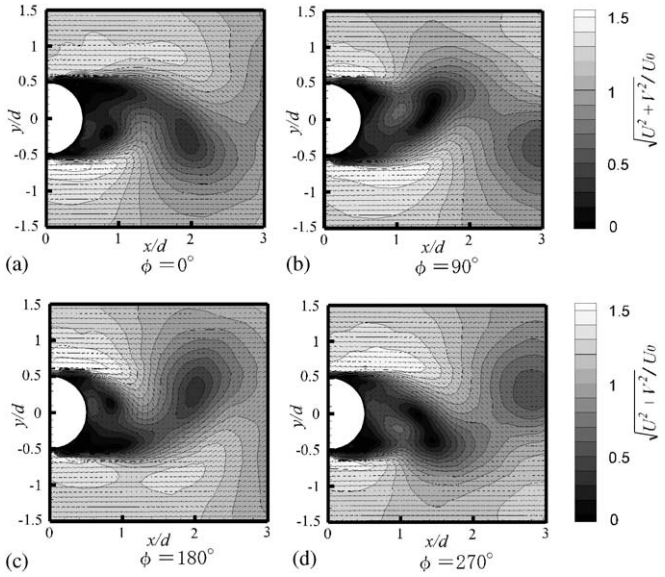

Fig. 5. Phase-averaged velocity magnitude for uncontrolled cylinder. (a) $\phi = 0°$, (b) $\phi = 90°$, (c) $\phi = 180°$, (d) $\phi = 270°$.

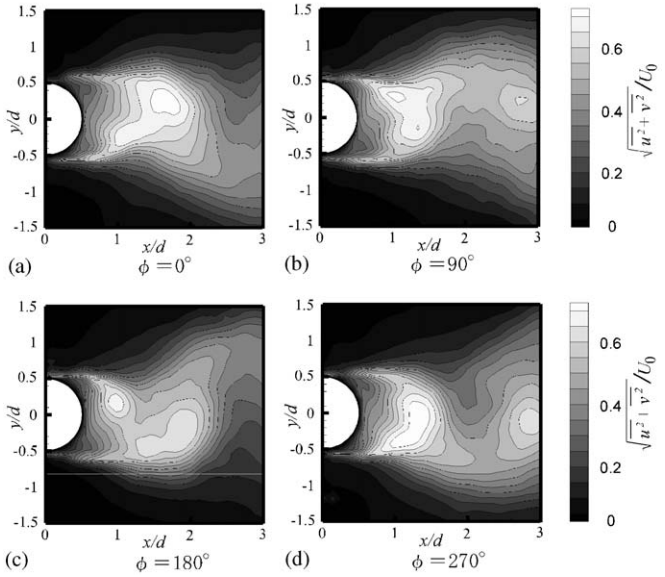

Fig. 6. Phase-averaged velocity fluctuations for uncontrolled cylinder. (a) $\phi = 0°$, (b) $\phi = 90°$, (c) $\phi = 180°$, (d) $\phi = 270°$.

the phase angle ϕ similar to those of the velocities in Fig. 5. It is mentioned that a highly turbulent region is created in the wake region ($x/d = 1 - 2$), where the wake deflection starts in the wake velocity field. The turbulent intensity of the highly turbulent region is over 60% of the free-stream velocity.

3.3. Observation of flow around controlled cylinder at vortex shedding frequency

Figs. 7(a)–(d) shows the phase-averaged velocity distribution around a circular cylinder under the acoustic excitation at four phase angles: $\phi = 0°$, 90°, 180°, 270°. The measurements are carried out at the condition of maximum drag reduction, where the control parameters are given by the forcing Strouhal number $S_f = 4S_{f0}$, the velocity amplitude $V_r = 1.5$ and the slit angle $\beta = 90°$. All the phase-averaged velocity distributions show that the wake region is elongated

downstream and its oscillation in the cross-flow direction is considerably weakened in comparison with those of the uncontrolled case. The cyclic variations of the flow field are only observed in the downstream region $x/d = 2-3$, where the two shear-layers merge at the centerline of the flow behind the cylinder. Therefore, the two shear layers develop downstream almost independently without the interaction. Such flow modification is due to the influence of acoustic excitation supplied through the slit. It is noted that such an elongation in the cylinder wake under acoustic excitation has been observed in the time-averaged velocity field by Fujisawa and Takeda (2003).

The corresponding phase-averaged velocity fluctuations around the circular cylinder under acoustic excitation are given in Fig. 8. Compared to those of the uncontrolled case, the magnitude of the velocity fluctuations and the cyclic behavior of the wake oscillation are substantially reduced by the influence of acoustic excitation. The highly turbulent region observed in the uncontrolled case is almost eliminated in the distribution under the influence of control, which suggests that the deflection motion of the cylinder wake is weakened by the control action. It is noted that the presence of the slightly turbulent region is observed only in the upper shear layer, which is due to the influence of the control flow itself developing from the slit. These observations indicate that both periodic and turbulent properties of the cylinder wake are considerably reduced by the influence of acoustic excitation supplied through the slit. However, the present observation does not indicate the mechanism of acoustic excitation control on the flow field. Therefore, the flow observation at the excitation frequency will be examined in the following section.

3.4. Observation of flow around controlled cylinder at excitation frequency

The phase-averaged velocity distributions at excitation frequency are measured in the wake of the circular cylinder under acoustic excitation control. It is noted that the excitation frequency is four times larger than the vortex shedding frequency. The phase-averaged velocity distributions at excitation frequency are shown in Figs. 9(a)–(d) at four phase angles: $\psi = 0^\circ$, 90°, 180°, 270°. It is to be mentioned that the phase ψ of acoustic excitation is defined by the angle where the periodic signal of acoustic excitation changes from the negative to the positive, which corresponds to the change from the suction phase to the injection phase of the control flow. The wake velocity distribution in the lower half of the cylinder behaves almost independently of the phases of acoustic excitation. On the other hand, the upper half of the wake velocity distribution shows periodic variations of the flow field along the upper shear layer. The phase $\psi = 0^\circ$ corresponds to the start of the injection velocity of the acoustic excitation from the slit on the cylinder. Hence, the high velocity is just beginning to generate near the upper side of the cylinder. At the same time, periodic variations of velocities are observed along the upper shear layer in the downstream, which correspond to the vortices generated in former cycles of excitations. The periodic occurrence of high velocity along the upper shear layer indicates the continuous modification of the wake flow by the acoustic excitation control. With the advance of the excitation phase to $\psi = 90^\circ$, the high velocity region expands over the upper side of the cylinder surface, which is due to the maximum injection velocity of the control flow from the slit. At the same time, the high velocity region along the upper shear layer moves downstream with the convection velocity of the shear layer. On the other hand, the suction velocity starts at the phase $\psi = 180^\circ$, so that the low velocity is created locally near the slit. The velocity field at $\psi = 270^\circ$ corresponds to the control flow at the maximum suction velocity at the slit. Therefore, the low velocity region prevails over the upper part of the cylinder and the vortices move further downstream.

The corresponding phase-averaged velocity fluctuations under acoustic excitation control are shown in Fig. 10. Although the distributions of the velocity fluctuations on the lower side of the cylinder are similar to the observation at vortex shedding frequency, the periodic structures of large velocity fluctuations appear clearly along the upper shear layer. It is found that the position of the large velocity fluctuations is located at the large velocity gradient just below the position of high velocity in Fig. 9. Therefore, the large velocity fluctuations in the upper shear layer are due to the influence of velocity field created by the acoustic excitation. The region of large velocity fluctuations moves downstream along the upper shear layer and merges with the velocity fluctuations from the lower shear layer at the centerline of the flow around the cylinder.

The vorticity distributions in the wake of the cylinder under the acoustic excitation control are evaluated from the phase-averaged velocity distributions. The result is shown in Figs. 11(a)–(d) at four phase angles: $\psi = 0^\circ$, 90°, 180°, 270°. The vorticity is defined by $\zeta = d/U_0(\partial V/\partial x - \partial U/\partial y)$, where counter-clockwise vorticity is positive and clockwise vorticity is negative. The negative vorticity is generated along the upper shear layer and the positive one is along the lower shear layer. It is noted that the upper shear layer consists of a series of discrete vortices, which are generated by the control flow from the slit on the upper side of the cylinder. The positions of these vortices agree with those of the large velocity gradient in Fig. 9 and the high velocity fluctuations in Fig. 10. Therefore, the velocity disturbances created by the acoustic excitation from the slit grow to form a series of discrete vortices along the upper shear layer. It is expected that the vortex structure along the upper shear layer is strengthened by the lock-in phenomenon of the shear layer, because the excitation frequency $4S_{f0}$ is expected to be in the effective range of synchronization of the shear-layer

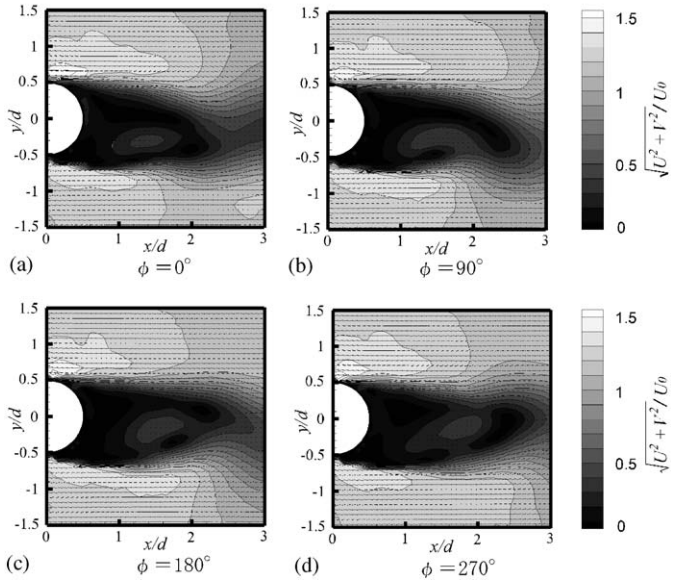

Fig. 7. Phase-averaged velocity magnitude under acoustic excitation at vortex shedding frequency. (a) $\phi = 0°$, (b) $\phi = 90°$, (c) $\phi = 180°$, (d) $\phi = 270°$.

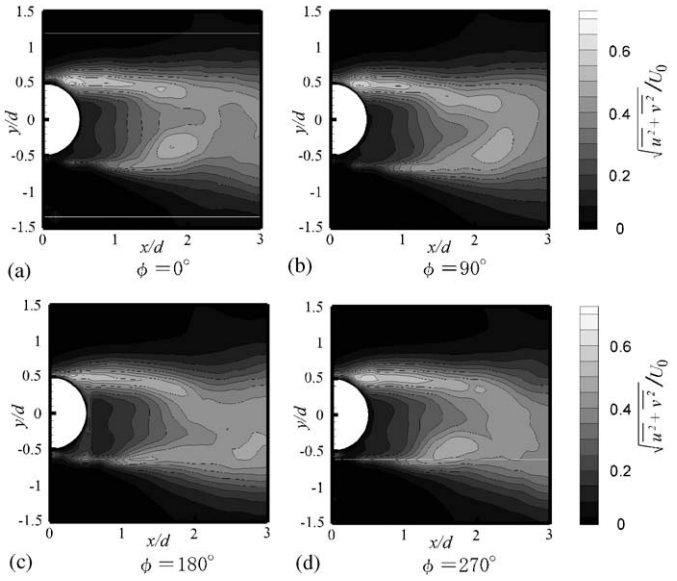

Fig. 8. Phase-averaged velocity fluctuations under acoustic excitation at vortex shedding frequency. (a) $\phi = 0°$, (b) $\phi = 90°$, (c) $\phi = 180°$, (d) $\phi = 270°$.

(Hsiao and Shyu, 1991), where the unstable frequency is estimated as $10.5S_{f0}$ at the Reynolds number Re = 9000 (Prasad and Williamson, 1996). This lock-in phenomenon along the upper shear layer modifies the flow structure in the cylinder wake and may lead to the reduction in shear-layer interaction.

It should be mentioned that the phase-averaged flow properties of the cylinder flow near the slit are studied at higher Reynolds numbers Re = 21500, where the slit is located at $\beta = 60°$ to correspond to the case of maximum drag reduction (Glezer et al., 2003). Their results indicate that a series of discrete vortices is generated over the cylinder surface interacting with the wall boundary layers, which leads to the modification of the surface pressure distribution

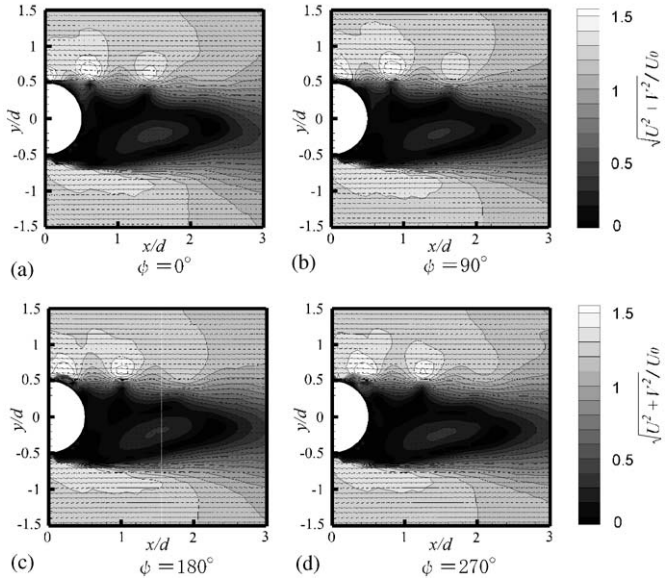

Fig. 9. Phase-averaged velocity magnitude under acoustic excitation at excitation frequency. (a) $\psi = 0°$, (b) $\psi = 90°$, (c) $\psi = 180°$, (d) $\psi = 270°$.

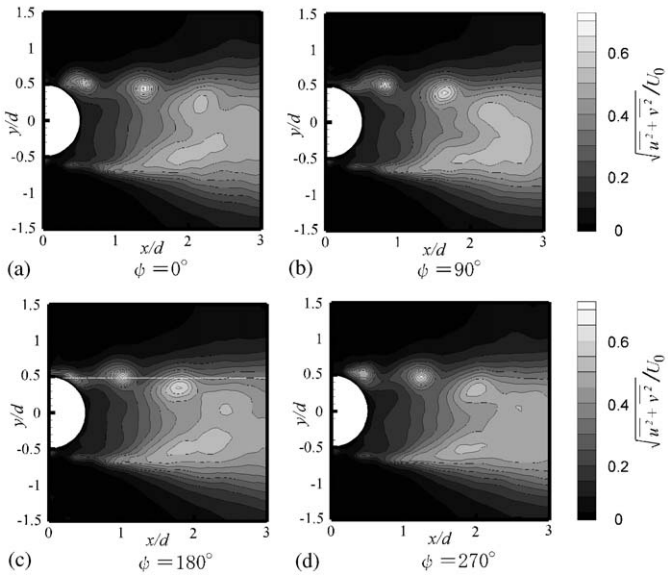

Fig. 10. Phase-averaged velocity fluctuations under acoustic excitation at excitation frequency. (a) $\psi = 0°$, (b) $\psi = 90°$, (c) $\psi = 180°$, (d) $\psi = 270°$.

and the delay in the separation point along the cylinder surface. Therefore, the acoustic excitation is very effective to modify the structure of the shear layer downstream of the slit over a wide range of Reynolds numbers.

3.5. Contour of cross-correlations in velocity fluctuations

In order to confirm the reduced interaction between the two shear layers of the cylinder wake, the cross-correlation coefficients of velocity fluctuations are evaluated in the present experiment. An example of the cross-correlation contour is shown in Figs. 12 and 13 for the uncontrolled and controlled case, respectively. Each figure shows the cross-

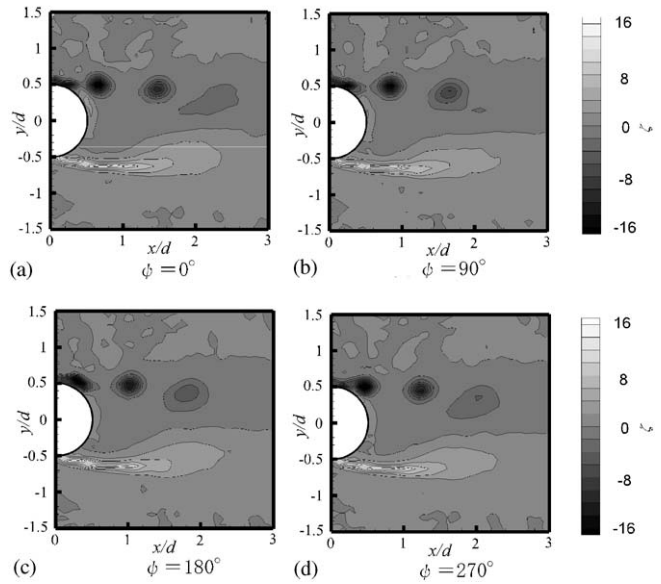

Fig. 11. Vorticity contour under acoustic excitation at excitation frequency. (a) $\psi = 0°$, (b) $\psi = 90°$, (c) $\psi = 180°$, (d) $\psi = 270°$.

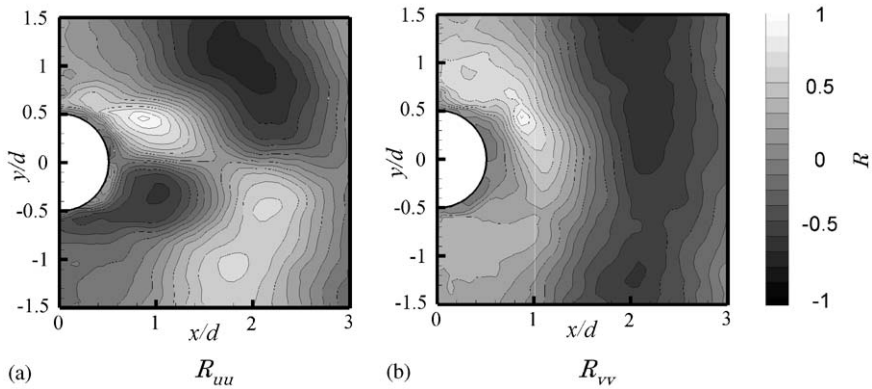

Fig. 12. Contour of cross-correlation coefficient for uncontrolled cylinder. (a) R_{uu}, (b) R_{vv}.

correlation coefficient between the streamwise velocity fluctuations R_{uu} and that between the normal velocity fluctuations R_{vv}. They are defined by

$$R_{uu} = \overline{u(x_0, y_0)u(x, y)} / \{u_{\text{r.m.s.}}(x_0, y_0)u_{\text{r.m.s.}}(x, y)\}$$

and

$$R_{vv} = \overline{v(x_0, y_0)v(x, y)} / \{v_{\text{r.m.s.}}(x_0, y_0)v_{\text{r.m.s.}}(x, y)\},$$

where u, v are streamwise and normal velocity fluctuations, respectively. The reference point x_0, y_0 is set to $x_0/d = 0.84$ and $y_0/d = 0.47$ in the upper shear layer of the cylinder wake. The contour of cross-correlations R_{uu} and R_{vv} of the uncontrolled case (Fig. 12) indicates the presence of highly correlated flow structures in the flow field, which is caused by the interaction of the two shear layers in the cylinder wake. When the acoustic excitation is applied to the flow field around the cylinder, the contour map (Fig. 13) shows the reduced correlation in the flow field. The highly correlated flow structure is observed only in the upper shear layer near the reference point, which indicates the formation of cyclic vortices along the upper shear layer by the velocity fluctuations of the control flow from the slit. This result also indicates that the interaction between the two shear layers in the wake of the cylinder is almost removed by the influence

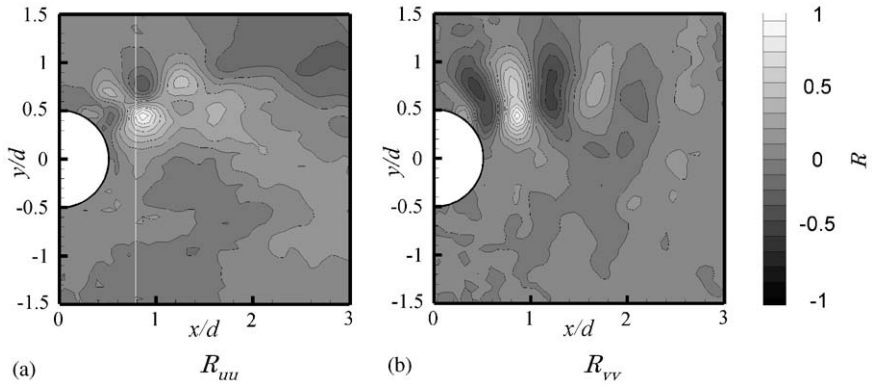

Fig. 13. Contour of cross-correlation coefficient for controlled cylinder. (a) R_{uu}, (b) R_{vv}.

of acoustic excitation control. Similar results were obtained when the reference points are shifted to other points in the cylinder wake.

4. Conclusions

The influence of the internal acoustic excitation on the aerodynamic performance of a circular cylinder in a uniform flow is studied by the phase-averaged measurements of the fluid forces and the PIV measurement of the flow field around the cylinder. It is found that the mean drag as well as the fluctuating lift are reduced by the influence of the acoustic excitation control. The phase-averaged PIV measurements at the vortex shedding frequency indicate that the periodic variations of the wake velocity field are weakened and the fluctuating velocities in the wake are considerably reduced in comparison with the uncontrolled case. These results support the improvement in the aerodynamic performance of the cylinder by the acoustic excitation control. On the other hand, the flow observation at the excitation frequency indicates the formation of discrete vortices along the shear layer by the action of flow control. The interaction of these vortices with the cylinder wake weakens the velocity correlations in the cylinder wake and results in the attenuation of the vortex shedding phenomenon and the improvement in the aerodynamic performance of the cylinder.

Acknowledgements

The authors would like to thank the reviewers and Prof. A. Glezer of Georgia Institute of Technology for their comments and suggestions.

References

Amitay, M., Honohan, A., Trantman, M., Glezer, A., 1997. Modification of the aerodynamic characteristics of bluff bodies using fluidic actuators. AIAA paper, 97–2004.

Bearman, P.W., 1984. Vortex shedding from oscillating bluff bodies. Annual Review of Fluid Mechanics 16, 195–222.

Blevins, R.D., 1985. The effect of sound on vortex shedding from cylinders. Journal of Fluid Mechanics 161, 217–237.

Blevins, R.D., 1990. Flow-induced Vibration, 2nd Edition. Van Nostrand Reinhold, New York, pp.43–103.

Drescher, H., 1956. Messung der auf querongesromte zylinder ausgeubten seitlich veranderten drucke. Zeitschrift fuer Flugwissensschaft 4, 17–21.

Ffowcs Williams, J.E., Zhao, B.C., 1989. The active control of vortex shedding. Journal of Fluids and Structures 3, 115–122.

Filler, J.R., Marston, P.L., Mih, W.C., 1991. Response of the shear layers separating from a circular cylinder to small-amplitude rotational oscillations. Journal of Fluid Mechanics 231, 481–499.

Fujisawa, N., Takeda, G., 2003. Flow control around a circular cylinder by internal acoustic excitation. Journal of Fluids Structures 17, 903–913.

Fujisawa, N., Ikemoto, K., Nagaya, K., 1998. Vortex shedding resonance from a rotationally oscillating cylinder. Journal of Fluids and Structures 12, 1041–1053.

Fujisawa, N., Kawaji, Y., Ikemoto, K., 2001. Feedback control of vortex shedding from a circular cylinder by rotational oscillations. Journal of Fluids and Structures 15, 23–37.

Glezer, A., Amitay, M., Honohan, A.M., 2003. Aspects of low- and high-frequency aerodynamic flow control, AIAA Paper 2003–0533.

Griffin, O.M., Hall, M.S., 1991. Review; vortex shedding lock-on and flow control in bluff body wakes. ASME Journal of Fluids Engineering 113, 526–537.

Gunzburger, M.D., Lee, H.C., 1996. Feedback control of Karman vortex shedding. ASME Journal of Applied Mechanics 63, 828–835.

He, J.-W., Glowinski, R., Metcalfe, R., Nordlander, A., Periaux, J., 2000. Active control and drag optimization for flow past a circular cylinder (1.Oscillatory cylinder rotation). Journal of Computational Physics 163, 83–117.

Hsiao, F.B., Shyu, J.Y., 1991. Influence of internal acoustic excitation upon flow passing a circular cylinder. Journal of Fluids and Structures 5, 427–442.

Kaga, A., Inoue, Y., Yamaguchi, K., 1994. Pattern tracking algorithms for airflow measurement through digital image processing of visualized images. Journal of the Visualization Society of Japan 14, 108–115 (In Japanese).

Naudascher, E., 1987. Flow-induced streamwise vibrations of structures. Journal of Fluids and Structures 1, 265–298.

Park, D.S., Ladd, D.M., Hendricks, E.W., 1994. Feedback control of von Karman vortex shedding behind a circular cylinder at low Reynolds numbers. Physics of Fluids 6, 2390–2405.

Prasad, A., Williamson, C.H.K., 1996. The instability of the separated shear layer from a bluff body. Physics of Fluids 8, 1347–1349.

Shiels, D., Leonard, A., 2001. Investigation of a drag reduction on a circular cylinder in rotary oscillation. Journal of Fluid Mechanics 431, 297–322.

Srinivas, K., Fujisawa, N., 2003. Effect of rotational oscillation upon fluid forces about a circular cylinder. Journal of Wind Engineering and Industrial Aerodynamics 91, 637–652.

Tokumaru, P.T., Dimotakis, P.E., 1991. Rotary oscillation control of a cylinder wake. Journal of Fluid Mechanics 224, 77–90.

Warui, H.M., Fujisawa, N., 1996. Feedback control of vortex shedding from a circular cylinder by cross-flow cylinder oscillations. Experiments in Fluids 21, 49–56.